European Journal of Pharmaceutics and Biopharmaceutics 142 (2019) 101–113

Contents lists available at ScienceDirect

European Journal of Pharmaceutics and Biopharmaceutics

journal homepage: www.elsevier.com/locate/ejpb

Research paper

The sub-chronic impact of $mPEG_{2k}$-PCL_x polymeric nanocarriers on cytochrome P450 enzymes after intravenous administration in rats

Qian Li[a], Minghui Sun[b], Genyun Li[a], Lihui Qiu[b], Zi Huang[a], Jingyi Gong[a], Jiangeng Huang[a], Gao Li[a], Luqin Si[a,*]

[a] Department of Pharmaceutics, School of Pharmacy, Tongji Medical College of Huazhong University of Science and Technology, 13 Hangkong Road, Wuhan 430030, PR China

[b] Department of Pharmaceutics, Affiliated Tongji Hospital, Tongji Medical College of Huazhong University of Science and Technology, 1095 Jiefang Avenue, Wuhan 430030, PR China

ARTICLE INFO

Keywords:
Polymeric micelles
Nano-carriers
$mPEG_{2k}$-PCL_x
Hepatic CYP450s
Induction
Pharmacokinetic properties
In vivo

ABSTRACT

Recent studies indicated obvious impacts of nano-carriers on cytochrome P450 enzymes (CYP450s) *in vitro*, but the effects *in vivo* are still unknown. In the present research, $mPEG_{2k}$-PCL_x micelles with different length of hydrophobic block (2000–10,000 Da) were intravenously administrated into rats for 14 days to evaluate the sub-chronic influences in the metabolic function of hepatic CYP450s. Although CYP1A1/B2 was susceptible to $mPEG_{2k}$-PCL_x micelles compared with other CYP isoenzymes, induction was mainly observed and varied with micelle type, administration dose, and CYP isoform. Interestingly, $mPEG_{2k}$-$PCL_{3.5k}$ micelles at 5 mg/kg increased the activity of CYP1A2, CYP2B1, CYP2C6, CYP2C11, and CYP3A1/2 while $mPEG_{2k}$-PCL_{5k} micelles only induced the latter three enzymes at 75 mg/kg. The mRNA expression of corresponding CYPs was mostly up-regulated by $mPEG_{2k}$-$PCL_{3.5k}$ micelles whilst less effect in protein level except for CYP3A1/2. Moreover, $mPEG_{2k}$-$PCL_{3.5k}$ micelles could affect the pharmacokinetic properties of phenacetin (CYP1A2), tolbutamide (CYP2C6), omeprazole (CYP2C11), and midazolam (CYP3A1/2) with a decrease of 19.6% in C_{max}, 20.5% in $AUC_{0\text{-}t}$, 31.6% in $AUC_{0\text{-}t}$, and 40.1% in C_{max} at 5 mg/kg, respectively ($P < 0.05$ or $P < 0.01$). These results unveiled nano-DDS might be involved in nanocarrier-drug interaction by intervening in the activity of CYP450s.

1. Introduction

In recent decades, diverse nanocarriers have been developed to delivery therapeutic active or diagnostic agents [1]. Nanoparticles (NPs) possess unique features that may improve the physicochemical properties of loading agents such as hydrophobicity and instability in the physiologic environment as well as pharmacokinetic characteristics like targeting distribution of diseased tissues and prolonging elimination from the body [2,3]. These promising merits are usually achieved by size-related effect and surface hydrophilicity of NPs, which makes it possible for drugs to show a better curative effect and significantly reduced side effects [4]. It is worth noting that most nanoparticles do not reach their intended target and 30–99% of administered dose will accumulate and sequester in the liver *in vivo* [5]. It's well known that most nanoparticles are taken by non-parenchymal cells despite 70–85% of the cells in the liver consisting of hepatocytes [5,6]. Strategies have been proposed to circumvent the phagocytosis of nanoparticles including surface modification, saturation of Kupffer cell phagocytic response, transient depletion of macrophages, and nanocarrier design from nature [5]. Nevertheless, the prolonged retention of nanoparticles also relatively slow clearance pathway and the associated concern of chronic toxicity to the liver parenchyma arise.

The liver is the largest internal organ of the body which performs various functions including detoxification, protein synthesis, and production of biochemicals necessary for digestion [7]. Metabolism of drugs and other xenobiotics in hepatic parenchyma plays a vital role in pharmaceutical toxicology. As is well known that the cytochrome P450 (CYP450) systems in liver constitute the largest and most important enzyme family involved in the detoxification and biotransformation of various endogenous/exogenous compounds [8]. As the special exogenous materials exposed *in vivo*, nanoparticles may be able to alter the metabolic activity of CYP450 enzymes. The effects of nanoparticles on CYP450 enzymes have been investigated including metallic, inorganic, and polymeric nano-carriers [9–11]. These studies mostly focused on

Abbreviations: Ahr, aryl hydrocarbon receptor; *Car*, constitutive androstane receptor; *Pxr*, pregnane X receptor; nano-DDS, nano- drug delivery system

* Corresponding author.
E-mail address: slq007@163.com (L. Si).

https://doi.org/10.1016/j.ejpb.2019.06.017
Received 25 February 2019; Received in revised form 9 June 2019; Accepted 17 June 2019
Available online 18 June 2019
0939-6411/

the *in vitro* inhibition or induction of NPs at microsomal systems or separated hepatocytes. The results indicated that the CYP450 enzymes were vulnerable to various NPs. However, whether this is the case in the body is still unclear. More exploration is needed to evaluate the interactions between nanoparticles and administrated drugs at a level of CYP450 enzymes *in vivo* model. It will contribute to profiling the influences of nanocarriers in hepatic metabolic function after co-administration of drugs and NP-based drug delivery systems.

The amphiphilic block copolymer consisting of a hydrophilic PEG and a hydrophobic PCL can spontaneously form into core-shell architectures which can encapsulate lipophilic drugs in the core while the shell can improve the *in vivo* pharmacokinetic properties [12,13]. PEG-PCL NPs are promising candidates as drug delivery tools characterized by high biocompatibility, biodegradability, and long-circulating features [14]. It has been widely accepted that micelles are rarely taken up by phagocytic cells for fewer serum proteins being absorbed to the PEG coating of NPs. The PEG-PCL micelles exhibit extended systemic circulation times lasting for more than 24 h or even days [15,16]. It has been also revealed that the micelles and unimers eventually accumulated in the liver and retained for a relatively long period of time [11,17]. Although *in vitro* studies indicated micelles might interfere in the function of CYP450 [11,18], studies relevant to the underlying mechanisms of micelles-induced effects on CYP450 enzymes and pharmacokinetic influence of CYP substrates are scarce in the literature. Accordingly, it deserves further investigation to identify the risks of micelle-drug interactions.

In this study, five $mPEG_{2k}$-PCL_x micelles with different molecular weights of PCL ranging from 2000 to 10,000 Da were used to elucidate the impact on CYP450 enzymes following by intravenous administration in SD rats. Changes in seven catalytic activities of major CYP450 enzymes (CYP1A1/B2, CYP1A2, CYP2B1, CYP2C6, CYP2C11, CYP2D2, and CYP3A1/2) were determined by comparing the concentration of metabolite from specific CYP450 enzyme probe substrate between the control group and $mPEG_{2k}$-PCL_x micelles treated groups in isolated rat liver microsomes (RLMs) *in vitro*. Furthermore, real-time polymerase chain reaction (RT-PCR) and Western blotting analysis were performed to evaluate the effects on mRNA level and protein expression of CYP450s, respectively. Specifically, pharmacokinetic profiles of probe substrates (amodiaquine for CYP1A1/B2, phenacetin for CYP1A2, bupropion for CYP2B1, tolbutamide for CYP2C6, omeprazole for CYP2C11, dextromethorphan for CYP2D2, midazolam for CYP3A1/2) were to evaluate the gradients in metabolic functions of CYP450s following i.v. administration of two doses of micelles for 14 days.

2. Materials and methods

2.1. Chemicals

$mPEG_{2k}$-PCL_x polymers were purchased from Jinan Daigang Biomaterial Co., Ltd. (Jinan, China), and all copolymers have been confirmed by ^1H NMR and FT-IR before use [19]. Amodiaquine, phenacetin, tolbutamide, omeprazole, 4-hydroxydiclofenac, 1-hydroxy midazolam, β-nicotinamide adenine dinucleotide phosphate disodium salt, D-glucose 6-phosphate disodium salt hydrate, and glucose-6-phosphate dehydrogenase were obtained from Sigma-Aldrich (St. Louis, MO, USA). Bupropion hydrochloride was from Shi Rui Technology (Wuhan, China). Diclofenac, dextromethorphan hydrobromide, midazolam, acetaminophen, dextrorphan, and propranolol were supplied by the National Institutes for Food and Drug Control (Beijing, China). N-desethyl amodiaquine, (S)-mephenytoin and 4-hydroxymephenytoin were provided by Toronto Research Chemicals Inc. (Toronto, ON, Canada). Hydroxybupropion was purchased from BD Biosciences (New York City, NY, USA). All the organic solvents of HPLC-grade were obtained from Fisher Scientific (Fair Lawn, NJ, USA).

2.2. Animals

Male Sprague-Dawley (SD) rats weighing 180–220 g were supplied by the Laboratory Animal Center of Tongji Medical College, Huazhong University of Science and Technology (Wuhan, China), housed at 22–25 °C, 50–60% humidity, and day/night cycle (12/12 h). Animals had access to food and water *ad libitum*. The Animal Ethics Committee of Huazhong University of Science and Technology (Wuhan, China) approved all experimental procedures.

2.3. Preparation and characterization of $mPEG_{2k}$-PCL_x micelles

$mPEG_{2k}$-PCL_x micelles were prepared by a slightly modified thin-film hydration method or nanoprecipitation method as described previously [11]. Briefly, $mPEG_{2k}$-PCL_{2k}, $mPEG_{2k}$-$PCL_{3.5k}$, and $mPEG_{2k}$-PCL_{5k} copolymers (150 mg) were dissolved in acetonitrile (ACN, 1 mL), respectively. After a layer of homogeneous film was formed at 50 °C for 2 h under vacuum rotary evaporation with a pressure of −0.1 MPa, the micellar suspensions were acquired by ultrasonic bath with 10 mM phosphate-buffered saline (PBS, pH 7.4) for 10 min. $mPEG_{2k}$-$PCL_{7.5k}$ and $mPEG_{2k}$-PCL_{10k} micelles were prepared by dropwise addition of polymer ACN solution (150 mg/mL) into PBS buffer (10 mM) and stirring overnight at ambient temperature. The residual organic solvent was evaporated under vacuum at 50 °C. Non-incorporated aggregates were removed by 0.22 μm membrane filters (polyethersulfone, PES). Particle sizes (nm), polydispersity index (PDI), and zeta potential (mV) of $mPEG_{2k}$-PCL_x micelles were measured by a ZetaPlus Zeta Potential Analyzer (Brookhaven Instrument Corporation, New York City, NY, USA) using 3 runs.

2.4. In vitro stability of $mPEG_{2k}$-PCL_x micelles in serum

The stability of PEG_{2k}-PCL_x micelles *in vitro* was evaluated in the presence of 90% fetal bovine serum (FBS) [20]. The volume ratio of micelle suspensions to 100% FBS was 1:9. The admixtures were incubated at 37 °C with gentle shaking at 30 rpm. Aliquots of 500 μL were removed at the different time points (1, 4, 8, 12, 24 h) for size measurement by a ZetaPlus Zeta Potential Analyzer (n = 3).

2.5. Hemolysis assay

The biocompatibility evaluation of $mPEG_{2k}$-PCL_x micelles was performed by hemolysis assay [21]. The erythrocytes were separated from 4 mL fresh heparinized blood (obtained from a single rat) by centrifugation at 2000 rpm for 5 min and washed with 16 mL PBS buffer until supernatant became achromatic. The depurative pellet was resuspended in PBS to obtain 2% erythrocyte suspension (v/v), which was mixed with $mPEG_{2k}$-PCL_x micellar suspension of various concentrations (0.25–2500 μg/mL) in equal volume, respectively. The mixture was incubated under shaking at 37 °C water bath for 3 h and centrifuged at 2000 rpm for 5 min. Hemoglobin release of the resulting supernatants was determined by a Synergy™ HT Multi-Mode Microplate Readers (Bio-Tek Instruments, Winooski, VT, USA) at 545 nm. The hemolysis percentage was calculated using the following equation:

$$\text{Hemolysis (\%)} = \frac{A_{sample} - A_{negative}}{A_{positive} - A_{negative}} \times 100\%$$

where A_{sample}, $A_{negative}$, and $A_{positive}$ were absorbance of the micellar sample, saline (0% hemolysis) and deionized water (100% hemolysis), respectively.

2.6. In vivo administration and sample collection

After 7 days of acclimatization, the rats were randomly divided into control and experimental groups (n = 3/group). The animals were

treated i.v. once daily for 14 consecutive days. In order to assess the *in vivo* effects on CYP450 enzymes, two different doses (5 and 75 mg/kg) were examined through calculating the initial blood concentration of micelles according to the clinical dose of the encapsulated drug and drug loading content from PEG-PCL-based drug carriers [22–24]. The control group was given with the same volume of PBS (10 mM, 5 mL/kg). Other groups were administered with five $mPEG_{2k}$-PCL_x micelles at 5 or 75 mg/kg/d (5 mL/kg), respectively. All rats were sacrificed under anesthesia of ether 24 h after the last treatment. Blood samples were drawn by cardiac puncture into heparinized tubes and centrifuged at 3500 rpm for 10 min to separate the plasma for determination of ALT and AST. The liver samples were quickly collected after perfusion with ice-cold PBS buffer (0.1 M, pH 7.4) containing KCl (0.15 M) to remove blood residue, 2 g of tissue was frozen in liquid nitrogen and stored at −80 °C for later oxidative stress assay, mRNA isolation, and protein extraction while the remaining specimen was divided for histologic assessment and preparation of microsomes.

2.7. Hepatic toxicity assay

Hepatotoxicity of $mPEG_{2k}$-PCL_x micelles was evaluated by assay of plasma biochemical levels including alanine aminotransferase (ALT) and aspartate aminotransferase (AST), assay of liver oxidative stress markers including glutathione (GSH) and reactive oxygen species (ROS), and histological analysis of liver tissues. According to the manufacturer's instructions, levels of ALT, AST, GSH, and ROS were determined by appropriate kits (Nanjing Jiancheng Bioengineering Institute, Nanjing, China) and a Synergy™ HT Multi-Mode Microplate Reader. Slices of liver tissues were fixed in 4% paraformaldehyde and embedded in paraffin blocks. Sections of 5 μm in thickness were prepared and then stained with hematoxylin–eosin (H&E). The histopathological changes were observed under a CX41 microscope (Olympus Corporation, Tokyo, Japan).

2.8. In vitro evaluation of CYP450 isoform activity in the liver

The activity of CYP450s was studied in the rat liver after administration of PBS or $mPEG_{2k}$-PCL_x micelles at dose levels (5 mg/kg/d and 75 mg/kg/d). Based on the results from the determination of CYP450 isoenzyme activity *in vitro*, the micelles which significantly affected the activity of CYP450 isoforms were then chosen to conduct real-time PCR analysis and Western blotting.

2.8.1. Preparation of rat liver microsomes

Rat liver microsomes (RLMs) were prepared by differential centrifugation method with some modification [25,26]. Briefly, liver samples were homogenized in 0.1 M PBS buffer (pH 7.4) containing 0.15 M KCl, 0.25 M sucrose, 10 mM Tris, 1 mM EDTA, and 1 mM PMSF. The homogenate was centrifuged at 10,000*g* for 20 min at 4 °C. The resulting supernatant was further centrifuged at 105,000*g* (Optima XPN-100, Beckman Coulter Inc., Fullerton, CA, USA) for 70 min. The microsomal pellet was resuspended with 2 mL of 0.1 M PBS buffer (pH 7.4, including 0.15 M KCl, 1 mM EDTA, 1 mM PMSF, and 20% glycerin) and stored at −80 °C before use. Protein concentrations in the microsomal fractions were determined by BCA method using a Synergy™ HT Multi-Mode Microplate Reader.

2.8.2. Determination of CYP450 isoenzyme activity

The activity of CYP1A1/B2, CYP1A2, CYP2B1, CYP2C6, CYP2C11, CYP2D2, and CYP3A1/2 was evaluated based on the concentration of metabolite from specific probe substrate in isolated rat liver microsomes referring to the previous method [11]. Briefly, the catalytic reactions were initiated by NADPH system and incubated with a specific substrate for a certain time after a 5 min pre-incubation period at 37 °C in a shaking water bath. The reactions were terminated by the addition of ice-cold ACN containing 50 ng/mL of propranolol as internal standard (IS). The incubation time and protein concentration for each CYP isoform were listed in Table 1. Three parallel samples were set for each rat. Subsequently, all samples were vortex-mixed for 3 min and centrifuged at 20,000 *g* (4 °C) for 10 min. The supernatant was collected for LC-MS/MS analysis. The activity of CYPs was represented as the percentage relative to the activity of the control group (% of control).

Table 1
Incubation conditions of hepatic microsomal CYP450 isozymes.

CYP450	Incubation time (min)	Protein concentration (mg/mL)
CYP1A1/B2	40	0.1
CYP1A2	30	0.2
CYP2B1	30	0.05
CYP2C6	10	0.1
CYP2C11	40	0.1
CYP2D2	15	0.1
CYP3A1/2	5	0.1

2.8.3. LC-MS/MS analysis

The LC-MS/MS system was composed of an API 4000 Qtrap® triple quadrupole mass spectrometer (AB Sciex, Foster City, CA, USA) connected to a Shimadzu Prominence UFLC (Shimadzu Corporation, Kyoto, Japan). The chromatographic separation was achieved on an ACQUITY UPLC® BEH C18 column (2.1 mm × 100 mm, 1.7 μm, Waters, Milford, MA, USA) coupled with an ACQUITY UPLC Col. In-Line Filter Kit (0.2 μm, Waters, Milford, MA, USA). The LC conditions and all MS/MS parameters were described previously [11]. Data were acquired and analyzed by Analyst 1.6.1 software (AB Sciex, Foster City, CA, USA).

2.9. RNA isolation, cDNA synthesis, and real-time PCR analysis

Total RNA was isolated from the frozen liver samples of $mPEG_{2k}$-$PCL_{3.5k}$ micelle group by TRIzol® reagent (Invitrogen, Carlsbad, CA, USA) according to the manufacturer's protocols. The concentration and quality of isolated RNA were verified by the 260/280 nm absorbance ratio (1.8–2.0 demonstrates highly pure samples) with a NanoDrop 2000c spectrophotometer (Thermo Scientific, Waltham, MA, USA). The first-strand cDNA products were generated using RevertAid First Strand cDNA Synthesis Kit (Thermo Scientific, Waltham, MA, USA) according to the manufacturer's instructions with a Veriti 96 Well Thermal Cycler (Applied Biosystems, Foster City, CA, USA). Thereafter, the effects of $mPEG_{2k}$-$PCL_{3.5k}$ polymeric micelles on gene levels of CYP450s were detected using real-time PCR analysis as our previous research [11]. The sequences of the primers used in the current study are shown in Table 2.

2.10. Western blotting analysis

Total protein was extracted from the hepatic tissue of $mPEG_{2k}$-$PCL_{3.5k}$ micelle-treated group by radio immunoprecipitation assay (RIPA) lysis buffer (Dalian Meilun Biotechnology Co., Ltd., Dalian, China) according to the manufacturer's protocols. Protein (50 μg) was separated by 10% sodium dodecyl sulfate-polyacrylamide gel electrophoresis (SDS-PAGE) and electro-transferred (100 V, 120 min) onto nitrocellulose membranes (Beijing Labgic Technology Co., Ltd., Beijing, China). The nitrocellulose membranes were blocked with 5% non-fat milk in TBST containing 150 mM NaCl, 10 mM Tris-HCl (pH 7.4) and 0.1% Tween 20 at room temperature for 80 min. Afterward, membranes were incubated overnight at 4 °C with primary antibodies, followed by rinsing three times with TBST at 10-min intervals. Incubation with appropriate secondary antibodies was performed for 1 h at ambient temperature. The antibody details were represented in Table 3. The bands were visualized on a Synergy GeneGnome5 chemiluminescence detection system (Synergy Co., Ltd., UK) using Clarity™ Western ECL Substrate (Bio-Rad, Hercules, CA, USA). The software imageJ2x

Table 2
Sequences of the primers used in real-time PCR analysis.

Genes	Forward primer	Reverse primer
Cyp1a1	TCAGACCCAACACTGGCATC	CAGCTCTTGGTCATCGTGGT
Cyp1a2	AATGTCATCGGAGCCATGTGT	GAAGTCCACAGCATTCCCTGA
Cyp2b1	TCATCGACACTTACCTTCTGC	GTGTATGGCATTTTACTGCGG
Cyp2c6	GACCTCATTCCTACCAACCT	CCTCTCCTGCACACATCC
Cyp2c11	ACATTGACACAACACCAGCTATCA	CAGGAATAAAACAAGCCTCGTAAAA
Cyp2d2	TGAGTGGCGAGAGCAGAG	CGAGCATAAACAAGGGAGG
Cyp3a1	GGAACTGCATTGGCATGAGG	TGCCAAGCAACTGTGAACTCT
Cyp3a2	AGTAGTGACGATTCCAACATAT	TCAGAGGTATCTGTGTTTCCT
Car	CATTTCCATGCCCTGACTTGTG	AGGCTGGACAATGGCGTCTC
Pxr	ATGTCTGATGCCGCTGTG	TGGAGGGAGGTTGGTAGTT
Ahr	GCCAATACGCACCAAAAGCA	TCGTCCTGTTGGATCAAGGC
Gapdh	GATGGTGAAGGTCGGTGTG	ATGAAGGGGTCGTTGATGG

(National Institutes of Health, Bethesda, MD, USA) was used to quantify the intensity of protein bands.

2.11. Pharmacokinetic study

A pharmacokinetic (PK) study was performed to demonstrate the influence of $mPEG_{2k}$-$PCL_{3.5k}$ micelles on *in vivo* disposition of specific substrates for CYP450 isoforms.

2.11.1. Experimental design

The rats were randomly divided into three groups (n = 12 per group): control multiple group (PBS), low-dose group (5 mg/kg), high-dose group (75 mg/kg). All animals were treated i.v. once daily for 14 days (5 mL/kg). After an overnight fasting period, rats in all groups were orally administrated with the cocktail substrates including amodiaquine (20 mg/kg), phenacetin (10 mg/kg), bupropion (10 mg/kg), tolbutamide (1 mg/kg), omeprazole (10 mg/kg), dextromethorphan (10 mg/kg), and midazolam (5 mg/kg) suspended in 0.5% CMC-Na (w/v) at a dose volume of 10 mL/kg. Blood samples (0.2 mL blood per time point) were drawn into heparinized tubes from the external jugular vein at pre-dose (0 h) and at 0.083, 0.25, 0.5, 0.75, 1, 1.5, 2, 3, 4, 6, 8, 12, 24 h postdose, followed by centrifugation at 3500 rpm for 10 min to separate plasma (about 0.1 mL) and stored at −80 °C before analysis.

2.11.2. Sample pretreatment and LC-MS/MS assay

All plasma samples were processed by protein precipitation method. An aliquot of 50 μL plasma was spiked with 150 μL ACN which contained 50 ng/mL of propranolol. The mixture was vortex-mixed for 3 min, followed by centrifugation at 20,000 *g* for 10 min (4 °C). A volume of 10 μL of supernatant was injected into the LC-MS/MS system for analysis under the same conditions described above.

2.11.3. PK analysis

The plasma concentration-time profiles were analyzed by a non-compartmental model and PK parameters including area under the plasma concentration-time curve from 0 to 24 h ($AUC_{0\text{-}t}$), maximum plasma concentration (C_{max}), clearance (CLz/F), time to reach C_{max} (T_{max}), and half-life ($t_{1/2}$) were obtained using Phoenix Winnonlin software (Version 6.4, Pharsight Corporation, Mountain View, CA, USA). The statistical analyses between the control group and the micelle-treated group were assessed with a two-tailed Student's *t*-test. A value of $P < 0.05$ was considered to be significant.

2.12. Statistical analysis

Data were represented as mean ± SEM. Statistical significance between multiple groups was evaluated using GraphPad Prism 7.0 software (GraphPad Inc., San Diego, CA, USA) followed by one-way ANOVA with a post-hoc Dunnett test. Differences were considered significant at $P < 0.05$.

3. Results

3.1. Characterization of micelles

As shown in Table 4, the $mPEG_{2k}$-PCL_x polymeric micelles with narrow and monodisperse unimodal patterns (PDI < 0.2) were successfully prepared by the thin-film method or nanoprecipitation method. The micellar hydrodynamic size varied from 20 to 100 nm in diameter with the increase of PCL molecular weight from 2000 to 10,000 Da. The zeta potential values indicated that the five $mPEG_{2k}$-PCL_x micelles were nearly neutral.

3.2. In vitro stability of $mPEG_{2k}$-PCL_x polymeric micelles in serum

The *in vitro* stability of $mPEG_{2k}$-PCL_x micelles in the presence of FBS showed that most micelles retained their particle size over a period of 24 h except $mPEG_{2k}$-PCL_{2k} micelles (Fig. 1). The size of $mPEG_{2k}$-PCL_{2k} micelles was changed after 1 h of adding FBS and increased to 55.0 nm with 24 h of incubation.

3.3. Hemolysis assay

The hemolytic profiles of $mPEG_{2k}$-PCL_x micelles after incubation with 2% erythrocyte suspension for 3 h were presented in Fig. 2. There was no obvious concentration-dependent manner in the hemolytic

Table 3
Primary and secondary antibodies used in the Western blotting analysis.

Name of antibody	Biological source	Species	Catalogue number	Company	Dilution ratio
Anti-CYP1A1	rabbit	human, mouse, rat	A2159	ABclonal[a]	1:1000
Anti-CYP1A2	mouse	human, mouse, rat	sc-53241	Santa Cruz[b]	1:500
Anti-CYP2B1	mouse	mouse, rat	sc-53244	Santa Cruz	1:500
Anti-CYP2C6	mouse	human, mouse, rat	sc-53245	Santa Cruz	1:500
Anti-CYP3A1	rabbit	human, mouse, rat	A1305	ABclonal	1:1000

[a] Wuhan, China.
[b] Dallas, USA.

Table 4
Particle size, PDI, and zeta potential of five polymeric micelles.

Polymeric micelles	Particle size (nm)	Polydispersity (PDI)	Zeta potential (mV)
$mPEG_{2k}$-PCL_{2k}	25.8 ± 0.3	0.053 ± 0.018	−0.35 ± 2.32
$mPEG_{2k}$-$PCL_{3.5k}$	44.3 ± 0.3	0.088 ± 0.013	−2.83 ± 14.34
$mPEG_{2k}$-PCL_{5k}	65.6 ± 0.7	0.178 ± 0.006	3.24 ± 5.27
$mPEG_{2k}$-$PCL_{7.5k}$	73.7 ± 2.4	0.025 ± 0.020	−1.79 ± 7.72
$mPEG_{2k}$-PCL_{10k}	97.2 ± 1.3	0.033 ± 0.002	−3.19 ± 12.32

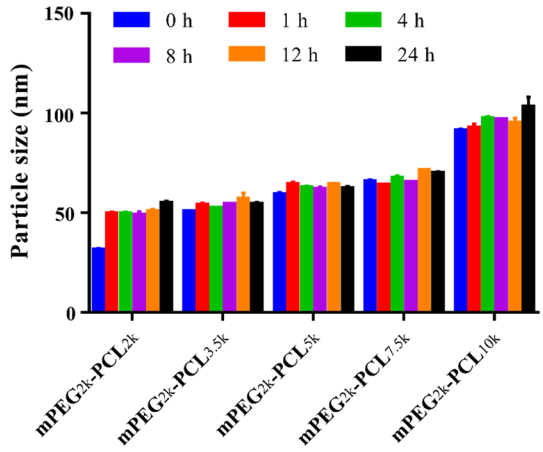

Fig. 1. Mean particle size of $mPEG_{2k}$-PCL_x micelles after incubation with FBS at various time points. Data are expressed as mean ± SEM (n = 3).

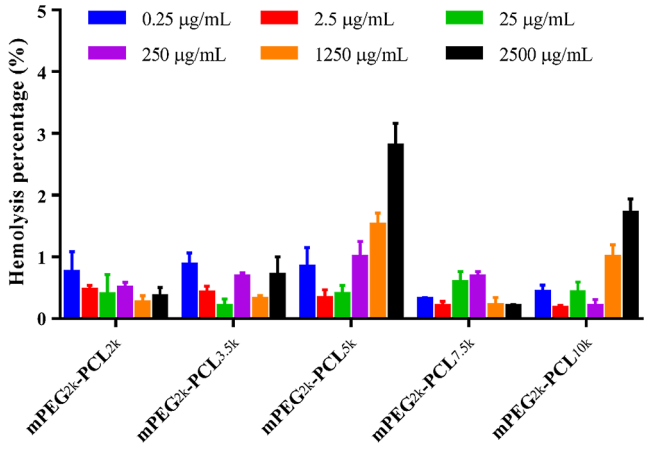

Fig. 2. Hemolytic profiles of $mPEG_{2k}$-PCL_x polymeric micelles at different concentrations. Data are expressed as mean ± SEM (n = 3).

activity of micelles except that the amount of hemolysis of $mPEG_{2k}$-PCL_{5k} and $mPEG_{2k}$-PCL_{10k} micelles tended to increase as the micellar concentration increased from 250 to 2500 μg/mL. Although $mPEG_{2k}$-PCL_{5k} micelles presented the highest hemolytic activity (2.8%), the hemolysis percentage was less than 5%, indicating that all five $mPEG_{2k}$-PCL_x micelles showed non-hemolytic activities [27].

3.4. Hepatic toxicity in vivo

Conferring to the results shown in Fig. 3A, plasma ALT ranging from 87% to 111% exhibited no statistically significant change in all $mPEG_{2k}$-PCL_x micelle-treated groups *vs* control group. Similar trends were observed for AST (Fig. 3B). The antioxidant system markers (GSH and ROS) were determined to evaluate the oxidative stress of rat liver *in vivo*. $mPEG_{2k}$-PCL_x micelles did not cause marked GSH depletion although treatment with $mPEG_{2k}$-PCL_{5k} at 75 mg/kg led to a slight decrease by 26% ($P > 0.05$, Fig. 3C). Results from Fig. 3D displayed no obvious differences in the hepatic levels of ROS for all treated groups. Hepatocytes from the microscopical observation were clear and intact (Fig. 3E). Compared to the control group, no obvious histopathological changes such as cell necrosis or replacement and tissue edema were examined in all micelle-treated groups.

3.5. Effect of $mPEG_{2k}$-PCL_x micelles on CYP450 activity in liver microsomes

Fig. 4 summarized the effect of different treatments on CYP450 activity in isolated rat liver microsomes. The incubation of liver microsomes from $mPEG_{2k}$-PCL_x micelle-treated rats with specific substrates of CYP450s resulted in a variety of effects depending on the CYP isoform, dose of micelle administration, and micelle type. Compared with other CYP isoforms, CYP1A1/B2 tended to be influenced by $mPEG_{2k}$-PCL_x micelles ($P < 0.01$ or $P < 0.001$). The transformation of N-desethylamodiaquine from amodiaquine by CYP1A1/B2 was significantly induced to 1.6-fold, 1.4-fold, 1.4-fold, and 1.3-fold in $mPEG_{2k}$-PCL_{2k} (5, 75 mg/kg), $mPEG_{2k}$-$PCL_{7.5k}$ (5 mg/kg), and $mPEG_{2k}$-PCL_{10k} micelle (75 mg/kg) groups, while marked decreases of 45.2% and 31.5% were observed in $mPEG_{2k}$-$PCL_{3.5k}$ (75 mg/kg) and $mPEG_{2k}$-PCL_{5k} (5 mg/kg) groups, respectively (Fig. 4A). Interestingly, high dose (75 mg/kg) of $mPEG_{2k}$-$PCL_{3.5k}$ micelles produced less impact on CYP450 activity in comparison with 5 mg/kg. However, treatment with $mPEG_{2k}$-PCL_{5k} micelles at 75 mg/kg significantly increased the activity of CYP2C6, CYP2C11, and CYP3A1/2 to 1.5-fold, 2.0-fold, and 1.5-fold, respectively. As to the type of polymeric micelles, $mPEG_{2k}$-$PCL_{3.5k}$ micelles at 5 mg/kg exerted remarkable induction effects ($P < 0.001$) on the activity of most CYP isoforms with the exception of CYP1A1/B2 and CYP2D2 while other micelles showed relatively fewer influences or even opposite effects. For example, the $mPEG_{2k}$-PCL_{10k} micelles had no obvious influences on the activity of CYP450 enzyme except CYP1A1/B2 whereas $mPEG_{2k}$-$PCL_{7.5k}$ micelles exhibited inhibitory effects or tendency on most CYP450 enzymes.

3.6. Effect of $mPEG_{2k}$-$PCL_{3.5k}$ micelles on mRNA expression

As $mPEG_{2k}$-$PCL_{3.5k}$ micelles exhibited considerable impact on the CYP450 activity after treatment for 14 days, mRNA levels of CYP genes and nuclear-receptors in liver tissues were quantified for the genetic mechanism of observed changes in CYP isoforms. There were no significant differences in the mRNA expression levels of *Cyp1a1*, *Cyp2c11* and *Cyp2d2* enzymes for $mPEG_{2k}$-$PCL_{3.5k}$ micelle-treatment groups (Fig. 5). $mPEG_{2k}$-$PCL_{3.5k}$ micelles markedly increased the *Cyp1a2* and *Cyp3a2* mRNA levels in both treatment groups. The *Cyp2b1* and *Cyp2c6* mRNA expression levels were evidently upregulated to 6.0-fold and 2.1-fold at 5 mg/kg, respectively, but the expression level of *Cyp3a1* was significantly increased to 2.3-fold only at 75 mg/kg. In comparison to the control group, mRNA levels of nuclear receptors showed remarkable upregulation ranging from 2.0-fold to 2.5-fold at both doses of micelles except the expression of *Car* mRNA at the dose of 75 mg/kg.

3.7. Effect of $mPEG_{2k}$-$PCL_{3.5k}$ micelles on protein levels

The protein levels of CYP isoforms which exhibited significant changes in the activity and mRNA expression were investigated for understanding the molecular mechanism. In compassion to control group, $mPEG_{2k}$-$PCL_{3.5k}$ micelles at 75 mg/kg were observed to significantly increase the CYP3A1 protein level to 1.9-fold with a tendency towards 21.6% enhanced CYP3A1 protein level at 5 mg/kg. The protein levels of CYP3A2 showed remarkable upregulation to around 1.5-fold in both groups ($P < 0.001$). However, no obvious changes in CYP1A1, CYP1A2, CYP2B1, and CYP2C6 protein content were detected at all tested groups (Fig. 6A and 6B).

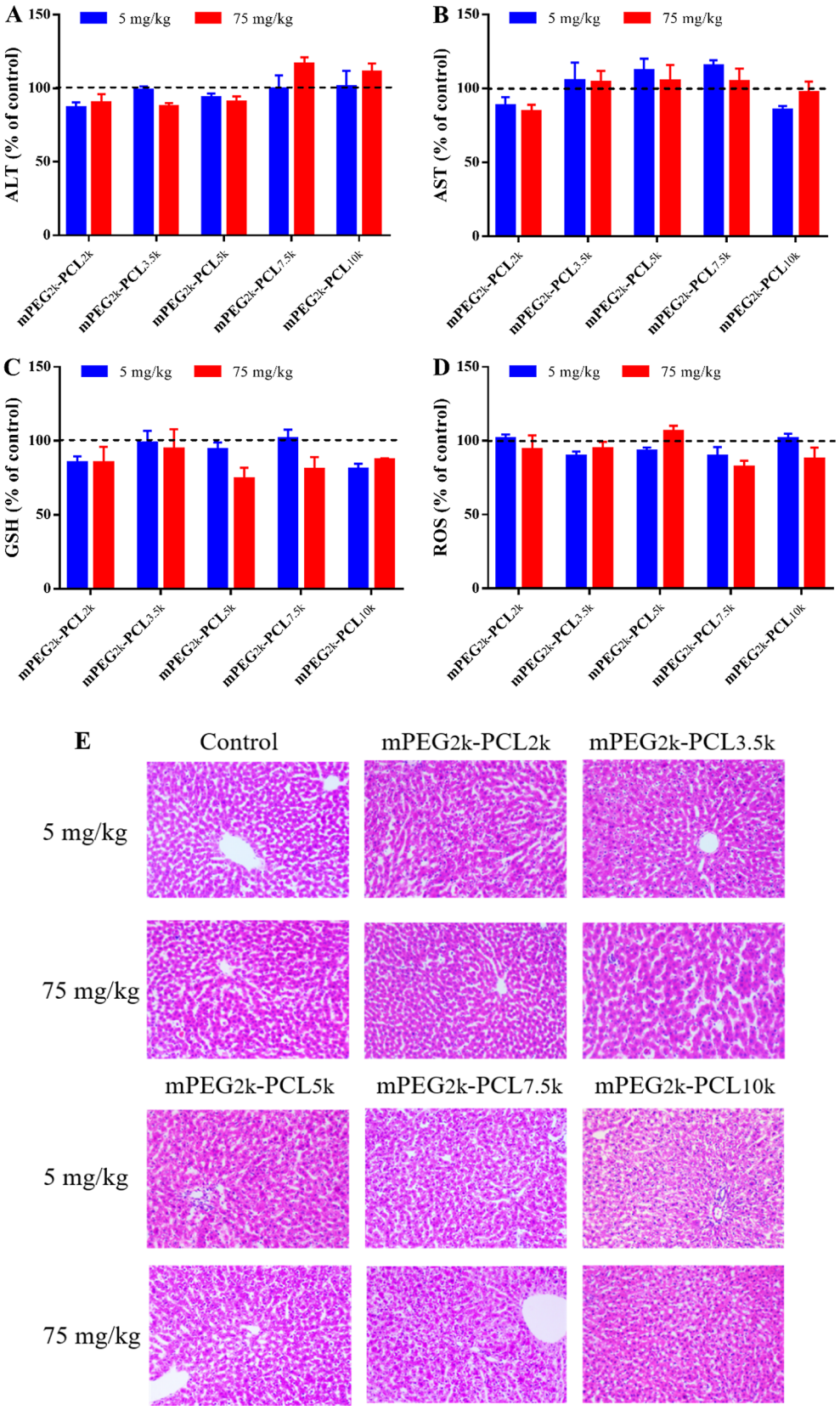

Fig. 3. Hepatoxicity of $mPEG_{2k}$-PCL_x polymeric micelles: the effects on the levels of ALT (A), AST (B), GSH (C), ROS (D), and histopathologic appearance of liver tissues (E) after i.v administration of micelles for 14 days. Data are expressed as mean ± SEM (n = 3).

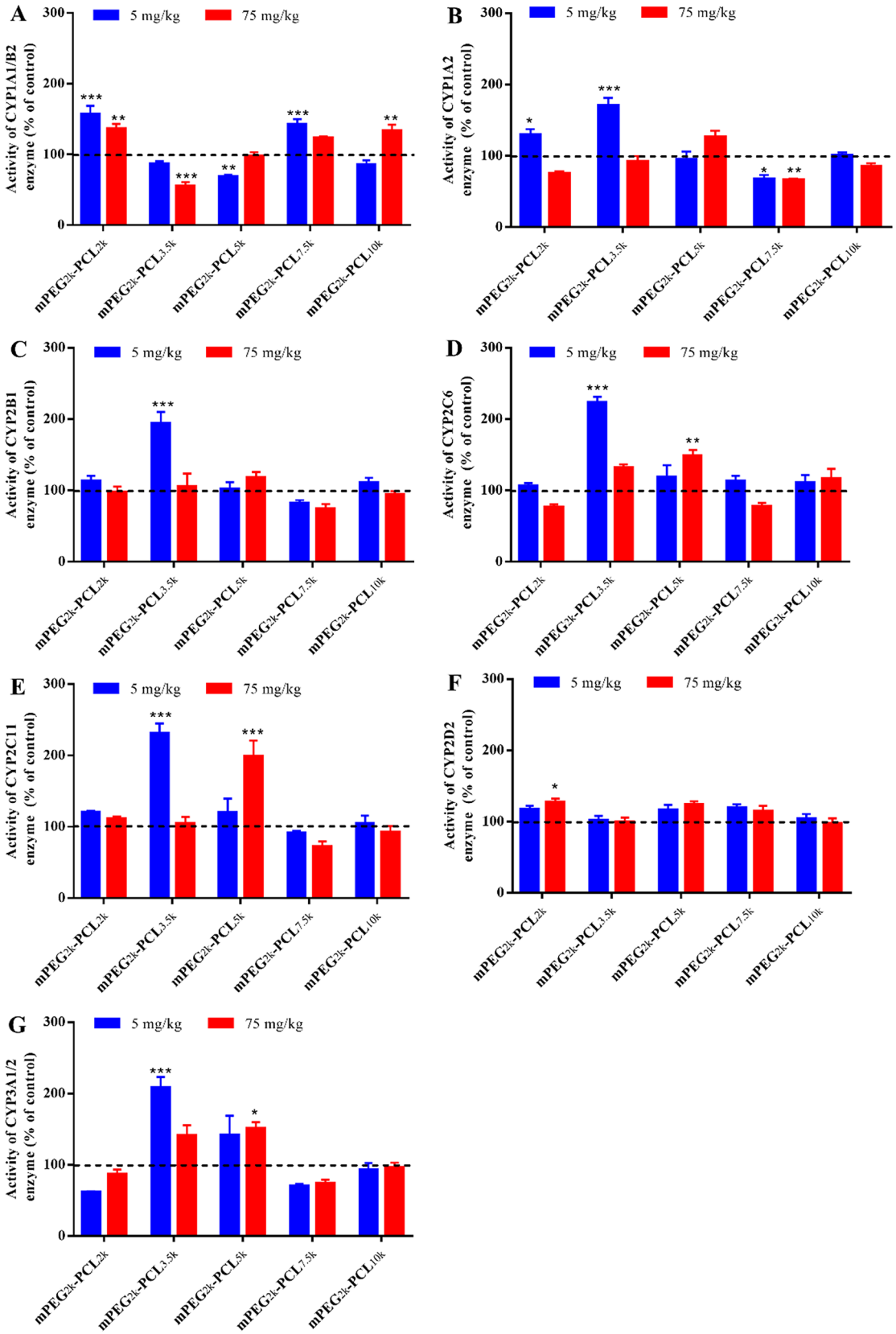

Fig. 4. Effect of $mPEG_{2k}$-PCL_x polymeric micelles on the activity of CYP1A1/B2 (A), CYP1A2 (B), CYP2B1 (C), CYP2C6 (D), CYP2C11 (E), CYP2D2 (F), CYP3A1/2 (G) in liver microsomes. Data are expressed as mean ± SEM (n = 3, and three parallel samples were set for each rat); $^{*}P < 0.05$, $^{**}P < 0.01$, $^{***}P < 0.001$ significantly different from the control group.

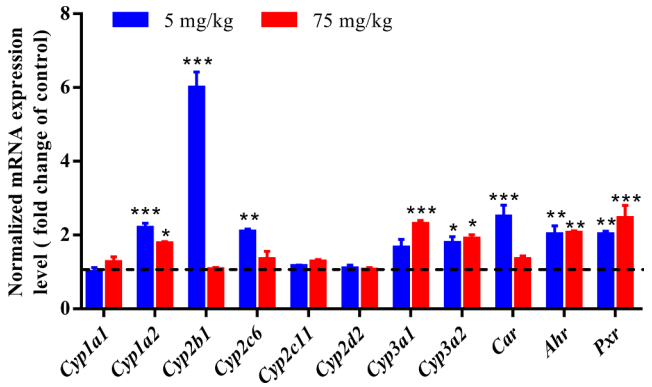

Fig. 5. Effect of mPEG$_{2k}$-PCL$_{3.5k}$ polymeric micelles on mRNA expression levels of CYP450s and nuclear receptors after i.v. administration for 14 days, respectively. Data are expressed as mean ± SEM (n = 3); $^{*}P < 0.05$, $^{**}P < 0.01$, $^{***}P < 0.001$ significantly different from the control group.

3.8. Effect of mPEG$_{2k}$-PCL$_{3.5k}$ micelles on PK in vivo

The PK parameters and mean plasma concentration-time curves of specific substrates were represented in Table 5 and Fig. 7. The C_{max} of phenacetin (substrate for CYP1A2) was significantly diminished by 19.6% and 17.1% ($P < 0.01$ or $P < 0.05$) for low dose and high dose micelle-treated groups, respectively. The $AUC_{0\text{-}t}$ and C_{max} of tolbutamide (CYP2C6) were also significantly decreased by 20.5% and 19.2% ($P < 0.05$) at 5 mg/kg, respectively. mPEG$_{2k}$-PCL$_{3.5k}$ micelles also remarkably suppressed the $AUC_{0\text{-}t}$ of omeprazole (substrate for CYP2C11) by 31.6% and 44.6% at 5 mg/kg and 75 mg/kg ($P < 0.05$ or $P < 0.01$), respectively. Moreover, the CLz/F in the low-dose and high-dose group was markedly augmented to 1.5-fold and 1.7-fold ($P < 0.05$ or $P < 0.001$), respectively. Although there were no significant differences in PK parameters, an accelerated trend towards the transformation of dextromethorphan (CYP2D2) was observed after treatment with micelles. The $AUC_{0\text{-}t}$ and C_{max} of dextromethorphan in the high-dose group were decreased by 30.0% and 26.1%, respectively; and the CLz/F was increased by 33.1% ($P > 0.05$). The $AUC_{0\text{-}t}$ and C_{max} of midazolam (CYP3A1/2) in the low-dose group were reduced by 28.4% ($P > 0.05$) and 40.1% ($P < 0.05$), respectively, while the CLz/F was enhanced to 1.3-fold ($P < 0.05$). However, mPEG$_{2k}$-PCL$_{3.5k}$ micelles showed no marked effects on the parameters of amodiaquine (CYP1A1/B2) and bupropion (CYP2B1) in all tested groups.

4. Discussion

In the present study, a series of mPEG$_{2k}$-PCL$_x$ micelles with the varied molecular weight of hydrophobic PCL segment were prepared and characterized to assess the effect of nano-carriers on metabolic function of CYP450 enzymes *in vivo*. The appropriate diameter (20–100 nm) of mPEG$_{2k}$-PCL$_x$ micelles make it possible to evade fast elimination by filtration of kidney and capture of the reticuloendothelial system (RES) [28,29]. The hydrophilic corona of micelles with neutral PEG shell could reduce absorption of serum proteins and stabilize the NP sizes over a period of 24 h (Fig. 1) although a certain length of the hydrophobic segment was suggested for maintaining stability from the results of mPEG$_{2k}$-PCL$_{2k}$ [15]. Semi-crystalline hydrophobic core of PCL may also contribute to enhancing the stability of micelles and lowering their interaction with membranes of blood cells [30]. All mPEG$_{2k}$-PCL$_x$ polymeric micelles ranging from 0.25 to 2500 μg/mL with < 5% of hemolysis percent (0.2–2.8%, Fig. 2) exhibited preferable hemocompatibility, compared with surfactants (amphiphilic compounds) which can destroy erythrocytes through penetration and saturation of cell membranes with unimers followed by solubilization of the membrane lipids and proteins at high concentrations [31].

It has been reported that NPs were mainly sequestered in the liver after administration into the body [5]. As earlier distribution studies showed that PEGylation could delay the uptake of nanoparticles by phagocytes, but mPEG$_{2k}$-PCL$_x$ could accumulate in the liver ultimately [11,30]. Moreover, repeated injection of micelles could saturate the sequestration of Kupffer cells and then the micelles might accumulate in the parenchymal cells through the fenestrae in the endothelial lining [32,33], The hepatic retention of NPs may result in histological changes accompanied by alterations of biochemical indices, depletion of GSH, and generation of ROS, which is often associated with inflammatory reaction [34]. Meanwhile, the elevated levels of inflammatory cytokines such as IL-6, IL-1β, INF-γ, and TNF could regulate hepatic CYP expression in inflammation [35,36]. There were no significant changes in biochemical markers (ALT, AST, GSH, and ROS) and histopathology of hepatic tissues (Fig. 3), which indicated negligible hepatotoxicity for the polymeric micelles, consistent with previous reports [22]. Thus, the mechanism of CYP450 activity induced by polymeric micelles is different from metallic and inorganic NPs which interact with proteins and enzymes of the hepatic tissue via interfering with the antioxidant defense mechanism and leading to ROS generation [37,38].

The activities of seven major CYP isozymes (CYP1A1/B2, CYP1A2, CYP2B1, CYP2C6, CYP2C11, CYP2D2, and CYP3A1/2) were

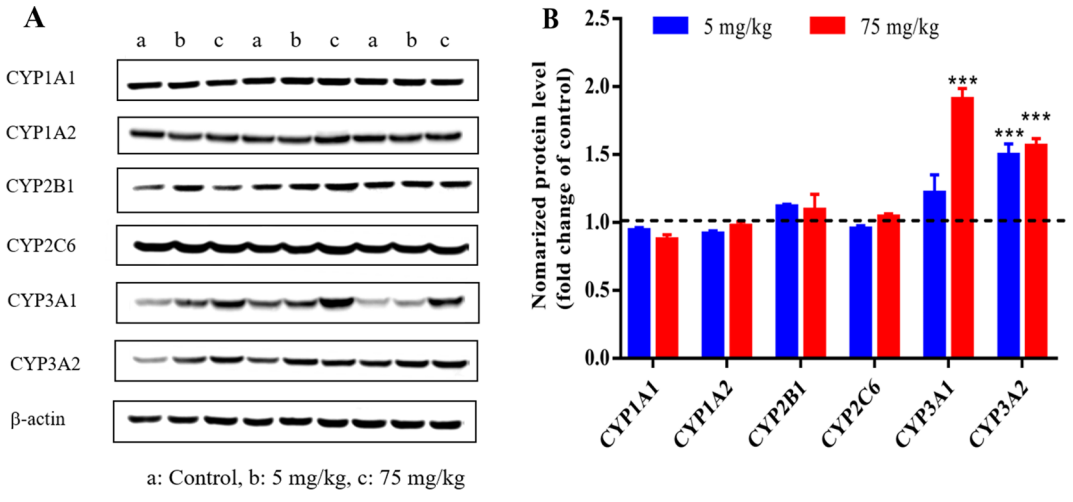

Fig. 6. Effect of mPEG$_{2k}$-PCL$_{3.5k}$ polymeric micelles on protein levels of CYP450 enzymes after i.v. administration for 14 days. Representative blots of three animals of each group were shown (A), and the quantification of blots for CYP450 enzymes was relative to the loading control (β-actin) (B). Data are expressed as mean ± SEM (n = 3); $^{***}P < 0.001$ significantly different from the control group.

Table 5
Main PK parameters of CYP450 substrates following oral administration to rats (n = 12, mean ± SEM).

Parameter	Control	5 mg/kg	75 mg/kg	Control	5 mg/kg	75 mg/kg
	Amodiaquine (CYP1A1/B2)			Phenacetin (CYP1A2)		
$AUC_{0\text{-}t}$ (μg·h/L)	217.1 ± 11.1	224.3 ± 14.3	228.4 ± 13.5	852.0 ± 63.8	772.5 ± 48.8	829.9 ± 48.7
C_{max} (μg/L)	32.8 ± 5.5	31.4 ± 2.8	38.1 ± 3.3	954.1 ± 50.1	767.2 ± 28.5**	791.1 ± 36.1*
CLz/F (L/h/kg)	81.9 ± 4.7	73.6 ± 3.0	72.7 ± 5.0	12.4 ± 0.9	13.4 ± 0.8	12.5 ± 0.9
T_{max} (h)	2.42 ± 0.45	2.29 ± 0.34	1.75 ± 0.27	0.35 ± 0.04	0.28 ± 0.03	0.27 ± 0.02
$t_{1/2}$ (h)	5.67 ± 0.48	7.94 ± 1.16	5.75 ± 0.51	0.34 ± 0.03	0.39 ± 0.04	0.44 ± 0.07
	Bupropion (CYP2B1)			Tolbutamide (CYP2C6)		
$AUC_{0\text{-}t}$ (μg·h/L)	464.6 ± 46.7	486.7 ± 34.2	473.0 ± 35.2	28694.0 ± 2199.0	22811.8 ± 1674.1*	26677.2 ± 1845.6
C_{max} (μg/L)	249.7 ± 24.7	234.7 ± 21.7	249.5 ± 9.5	2318.8 ± 137.4	1874.7 ± 143.1*	2322.4 ± 183.0
CLz/F (L/h/kg)	22.4 ± 2.4	21.4 ± 1.4	21.9 ± 1.5	0.032 ± 0.003	0.038 ± 0.004	0.035 ± 0.003
T_{max} (h)	0.83 ± 0.11	0.67 ± 0.06	0.59 ± 0.08	2.58 ± 0.57	1.61 ± 0.32	1.71 ± 0.45
$t_{1/2}$ (h)	1.64 ± 0.14	1.79 ± 0.19	1.38 ± 0.11	8.12 ± 0.75	10.55 ± 0.65*	8.22 ± 0.65
	Omeprazole (CYP2C11)			Dextromethorphan (CYP2D2)		
$AUC_{0\text{-}t}$ (μg·h/L)	353.6 ± 42.9	242.0 ± 23.5*	195.8 ± 18.0**	376.5 ± 45.4	398.9 ± 42.9	263.6 ± 37.6
C_{max} (μg/L)	331.0 ± 47.2	296.8 ± 29.4	238.9 ± 26.9	189.5 ± 21.2	166.8 ± 18.7	140.0 ± 18.3
CLz/F (L/h/kg)	30.2 ± 2.4	44.3 ± 4.9*	52.5 ± 5.1***	30.2 ± 5.8	27.1 ± 3.5	40.2 ± 4.6
T_{max} (h)	0.31 ± 0.04	0.30 ± 0.04	0.24 ± 0.01	0.75 ± 0.07	0.83 ± 0.12	0.56 ± 0.08
$t_{1/2}$ (h)	1.17 ± 0.20	1.21 ± 0.27	1.58 ± 0.29	1.96 ± 0.33	2.14 ± 0.21	1.77 ± 0.23
	Midazolam (CYP3A1/2)					
$AUC_{0\text{-}t}$ (μg·h/L)	246.9 ± 36.5	176.8 ± 17.2	209.0 ± 18.3			
C_{max} (μg/L)	205.6 ± 32.8	123.2 ± 14.7*	156.2 ± 15.6			
CLz/F (L/h/kg)	21.1 ± 2.1	28.1 ± 2.5*	24.2 ± 3.0			
T_{max} (h)	0.52 ± 0.06	0.40 ± 0.06	0.53 ± 0.07			
$t_{1/2}$ (h)	1.19 ± 0.25	1.65 ± 0.28	1.58 ± 0.24			

* Significantly different from the control group, $P < 0.05$.
** Significantly different from the control group, $P < 0.01$.
*** Significantly different from the control group, $P < 0.001$.

determined to evaluate the influences of micelles in hepatic metabolic function after intravenous administration in rats. The CYP isoforms of rats selected in present work have been reported in previous studies that they were corresponding with CYPs in human [11,26,39]. Rat CYP2D1 and CYP2D2 are considered to be corresponding with human CYP2D6 with homology by 71% [40], but the substrate specificity of CYP2D2 is most similar to that of human CYP2D6 in various models [26,41]. In addition, dextromethorphan, which usually was applied to assess the CYP2D6 activity, was metabolized specifically by CYP2D2 in male rats [39,42]. Consequently, rat CYP2D2 isoform other than CYP2D1 was chosen to evaluate the metabolism of probe substrate. Of note, drug metabolization and CYP isoenzyme expression differ between rat CYP3A1 and human CYP3A4. Although marked relevance has been revealed between rat CYP3A1 and human CYP3A4 [43], the rat orthologous CYP3A1 (the main CYP3A form in rats) is also not induced by rifampicin (a typical CYP3A4 inducer) and some prototypical substrates of human CYP3A enzymes are not metabolized by rat CYP3A1 [44]. Moreover, identical CYP3A4 enzyme is expressed in human liver and intestine, but CYP3A1 is mainly presented in liver for rats and CYP3A-mediated activities are also much higher in human than rat in intestines [45,46]. These differences could lead to overestimation or underestimation of DDI when extrapolating from rat to human. As CYP3A4 expressed in human liver and intestine with higher activities has a broader substrate specificity including 50% of therapeutic drugs currently in the market, the CYP3A-related interactions in rats still deserve further attention.

$mPEG_{2k}$-PCL_x micelles exerted different effects on the metabolic activities of CYP450 enzymes depending on types and concentrations of micelles which highly related to the characteristics of NPs (Fig. 4). Size of nanocarriers and hydrophobicity play essential roles in the interaction between NPs and proteins [47]. Smaller particle size providing more enhanced extra flexibility and surface area facilitates the interaction between nanoparticles and proteins [48,49]. Nevertheless, the $mPEG_{2k}$-PCL_{2k} micelles with the smallest hydrodynamic diameter showed less influence in CYP activity which might be attributed to increasing in size after incubation with FBS. Ukawala et al. also demonstrated that there was a more significant increment in the particle size of $mPEG_{2k}$-PCL_{2k} micelles from 36.1 nm to 301.7 nm in presence of bovine serum albumin (BSA) for 48 h while other $mPEG_{2k}$-PCL_x micelles remained unchanged [15]. Although changed bio-medium containing diverse serum proteins and concentrations will differ the alteration extent of particle size, the absorption of proteins and increasing size reduced the bioaccumulation in hepatocytes [50,51]. In addition, increased hydrophobicity is capable of augmenting protein affinity [52]. However, the increased protein affinity could be offset by the adhesion capacity of smaller micellar size [11]. Therefore, the result that $mPEG_{2k}$-$PCL_{3.5k}$ and $mPEG_{2k}$-PCL_{5k} micelles exerted marked induction on the metabolic activities of most CYP450s may account for the combination of micellar size and hydrophobicity. Moreover, the thermodynamically stable micelles (i.e. concentration of copolymer above CMC prior to and upon dilution following i.v. administration) were more effectively entrapped within the extracellular or vascular space of liver, while thermodynamically unstable micelles (i.e. concentration of copolymer above CMC prior to but not following dilution on i.v. administration) showed significant degree of intracellular uptake [16]. Finally, $mPEG_{2k}$-$PCL_{3.5k}$ at a higher micellar dose producing limited effects on CYPs may be accounted for aggregation owing to the formation of inter-particle bridges by the protein [53].

CYP450 enzymes are apt to inhibition by various NPs with microsomal systems *in vitro*, whilst it's hard to find the correlation between *in vitro* and *in vivo* [54]. Induction of CYP isoforms was mainly observed after administration of $mPEG_{2k}$-PCL_x for 14 days while inhibition was presented at higher concentration levels of micelles from microsome incubation *in vitro* in our previous work [11]. It's worth noting that a similar inductive tendency to CYPs in rat primary hepatocytes treated with $mPEG_{2k}$-PCL_x for 72 h and isolated liver microsomes after 14 days' treatments *in vivo*. However, inconsistency still existed. For example, $mPEG_{2k}$-PCL_x resulted in a general increase in the activity of CYP2B1 and 3A1/2 in primary hepatocytes *in vitro* while the micelles with a longer segment of PCL (*i.e.* $PCL_{7.5k}$ and PCL_{10k}) showed no or less induction. One possibility is that diverse factors such as dilution, degradation as well as the relatively low dose of NPs lead to less

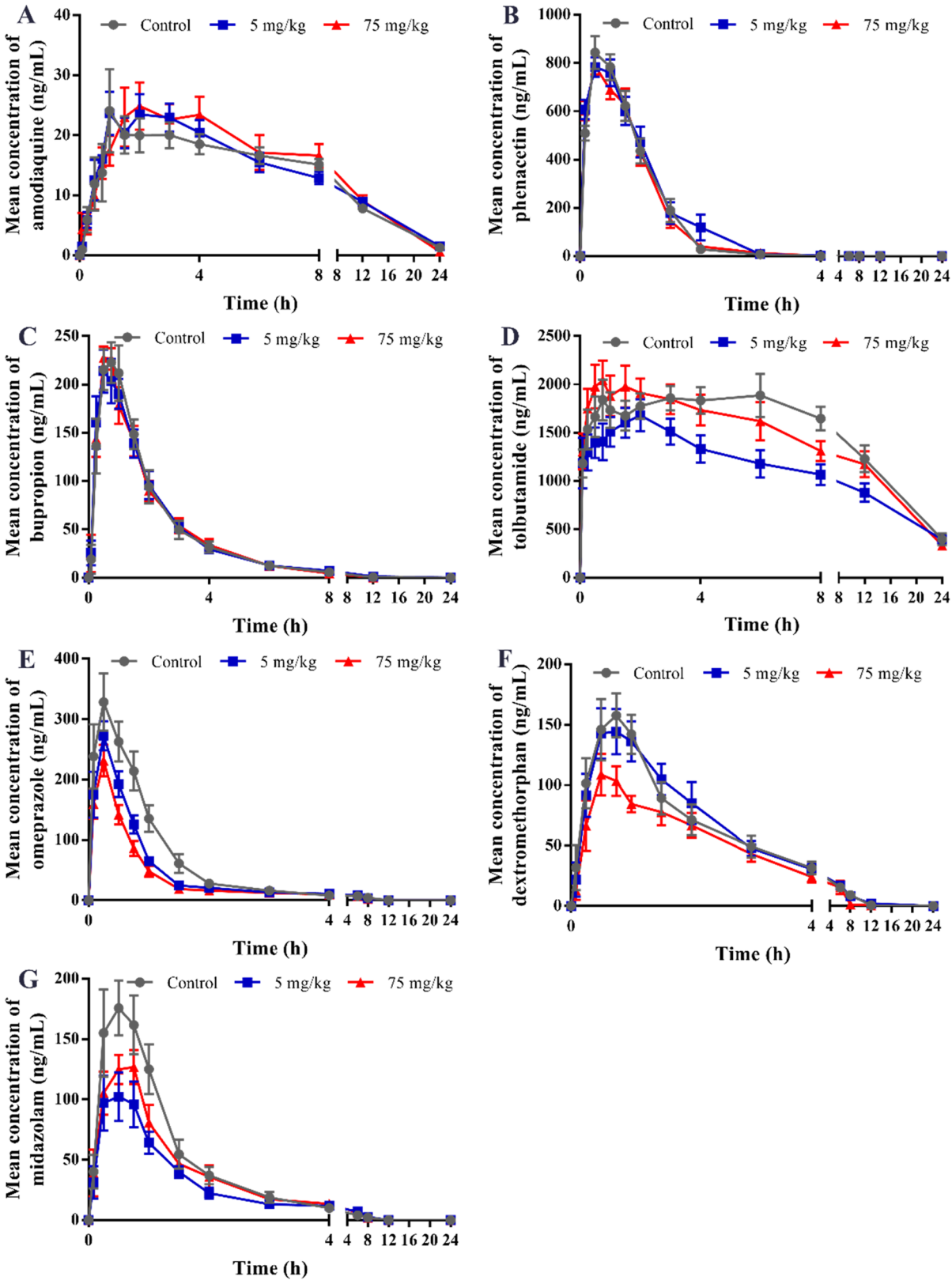

Fig. 7. Mean plasma concentration-time curves of amodiaquine (A), phenacetin (B), bupropion (C), tolbutamide (D), omeprazole (E), dextromethorphan (F), and midazolam (G) after multiple doses of intravenous $mPEG_{2k}$-$PCL_{3.5k}$ polymeric micelles in rats. Data are expressed as mean ± SEM (n = 12).

accumulation in hepatocytes in comparison of *in vitro* incubation system [22,32,55]. This also can be corroborated by the *in vivo* performance of $mPEG_{2k}$-PCL_{10k} with no significant effects on CYP activity for the larger micellar size. In addition, the length of the treatment may be involved in the adjustment of activity by regulating the mRNA levels and protein expression. Further investigation of exposure to NPs for a shorter or longer duration of *in vivo* is recommended in the future.

A cocktail approach was applied in the pharmacokinetic study with

Table 6
Summary of the effects of $mPEG_{2k}$-$PCL_{3.5k}$ micelles on the activity, mRNA level, protein expression and pharmacokinetics of probe substrates for CYP450 enzymes.

		CYP1A1/B2	CYP1A2	CYP2B1	CYP2C6	CYP2C11	CYP2D2	CYP3A1	CYP3A2
5 mg/kg	Activity	–	↑ (by 70.2%)	↑ (by 94.4%)	↑ (by 123.1%)	↑ (by 131.3%)	–	↑ (by 108.1%)	
	mRNA	–	↑ (by 119.2%)	↑ (by 498.7%)	↑ (by 109.0%)	–	–	(↑, by 65.7%)	↑ (by 78.4%)
	Protein	–	–	–	–	/	/	(↑, by 21.6%)	↑ (by 49.4%)
	Pharmacokinetics	AUC-, C_{max}-	AUC, C_{max}↓ (by 19.6%)	AUC-, C_{max}-	AUC↓, C_{max}↓ (by 20.5% and 19.2%)	AUC↓, C_{max}- (by 31.6%)	AUC-, C_{max}-	AUC(↓), C_{max}↓ (by 28.4% and 40.1%)	
75 mg/kg	Activity	↓ (by 45.2%)	–	–	(↑, by 32.1%)	–	–	(↑, by 40.9%)	
	mRNA	(↑, by 26.2%)	↑ (by 77.2%)	–	(↑, by 34.5%)	/	–	↑ (by 129.7%)	↑ (by 89.7%)
	Protein	–	–	–	–	/	/	↑ (by 90.6%)	↑ (by 56.2%)
	Pharmacokinetics	AUC-, C_{max}-	AUC, C_{max}↓ (by 17.1%)	AUC-, C_{max}-	AUC-, C_{max}-	AUC↓, C_{max}(↓) (by 44.6% and 27.8%)	AUC(↓), C_{max}(↓) (by 30.0% and 26.1%)	AUC-, C_{max}(↓) (by 24.0%)	

↑, ↓ significant increase or decrease ($P < 0.05$ or $P < 0.01$ or $P < 0.001$), respectively; – no change; (↑), (↓) a tendency to increase or decrease when ≥20% difference to the control group, respectively; / no investigation.

highly sensitive and specific substrates for reducing the number of animals and investigating the activities of multiple CYP activities in the same group. Reducing the administration doses was utilized to lower the concentrations of the substrates for minimizing the interactions between substrates representing the most challenging issue in the cocktail approach [56], though the potential interactions may still exist to a certain extent. Although there was no proportional correlation between PK parameters (*AUC* and C_{max}) and activity of CYP450 enzymes or the corresponding mRNA expression, the influence in pharmacokinetic profiles by $mPEG_{2k}$-$PCL_{3.5k}$ micelles was basically consistent with the tendency of activity and mRNA expression to increase (summarized in Table 6). Notably, treatment with multiple doses of $mPEG_{2k}$-$PCL_{3.5k}$ micelles exerted inductive effect or tendency on the metabolic function of CYP1A2, CYP2C6, CYP2C11, CYP2D2 and CYP3A1/2 from the results of reducing the exposure of substrate *in vivo*, consistent with the increased activities in isolated rat liver microsomes except that micelles at high dose exhibited more enhanced induction on CYP2C11. In line with rarely being induced by other xenobiotics for CYP2C11 and CYP2D2, the gene expression of these two enzymes could not be augmented by micelles [57,58]. However, $mPEG_{2k}$-$PCL_{3.5k}$ micelles have been shown to significantly regulate the mRNA expression of CYP1A2, CYP2C6, and CYP3A, which coincided with the increased isoenzyme activity. These findings indicated that polymeric micelles could alter the function of CYPs via adjusting the genetic levels. Moreover, the master transcriptional regulators of CYP450 enzymes were also related to the increased activity of CYPs. The elevated level of *Cyp1a2* may be involved in the *Ahr*-mediated transcriptional upregulation and the increased levels of *Cyp2b1*, *Cyp2c6*, and *Cyp3a1/2* were mostly consistent with the augmented mRNA level of *Car* and *Pxr* [59]. It's worth mention that $mPEG_{2k}$-$PCL_{3.5k}$ micelles exhibited less influence in the protein expression of the above enzymes except for CYP3A. The discrepancy might be attributed to the fact that the protein levels could be regulated at different processes including pre-translation, translation and post-translational modifications involved in epigenetic studies [60]. In addition, the relatively low proportion of these CYP isoenzymes in the liver might result in the insensitive of discriminating at protein levels because of the limits of western-blot analysis that the detection specificity of western blot largely depends on the quality of the antibodies and performance of the conjugated horseradish peroxidase, especially for low abundance proteins [61,62]. As for CYP3A enzyme with abundant content in the liver, the $mPEG_{2k}$-$PCL_{3.5k}$ micelles consistently exerted a marked increase in the activity, mRNA expression, and protein levels of CYP3A1/2.

5. Conclusions

This study was aimed to investigate the sub-chronic influences of nanocarriers in hepatic CYP450s after administration of $mPEG_{2k}$-PCL_x micelles to rats for 14 days. It was found that $mPEG_{2k}$-PCL_x micelles exerted different effects on the metabolic activities of CYP450s, which were relevant to the CYP450 isoform, micellar type, and administration dose. The CYP1A1/B2 was susceptible to $mPEG_{2k}$-PCL_x micelles compared with other CYP isoforms. The $mPEG_{2k}$-$PCL_{3.5k}$ micelles at 5 mg/kg showed remarkable induction effects ($P < 0.001$) on the activity of most CYP isoforms (CYP1A2, CYP2B1, CYP2C6, CYP2C11, and CYP3A1/2) which related to the mRNA expression of corresponding enzymes except for CYP2C11 isoenzyme. The polymeric micelles also accelerated the transformation of CYP substrates leading to a marked decrease in PK parameters C_{max} or *AUC* for CYP1A2, CYP2C6, CYP2C11 and CYP3A1/2 although there was no significant difference for substrate of CYP2D2. Our findings revealed that polymeric micelles might be involved in nanocarrier-drug interaction by intervening in the activity of CYP450s. This research will contribute to a better understanding of *in vivo* performances when therapeutic agents mainly metabolized by CYP450s were co-administered with NP formulations.

Declaration of Competing Interest

The authors have declared that there is no conflict of interest in this work.

Acknowledgements

This work was supported by National Natural Science Foundation of China, China (No. 81473170).

References

[1] A. Alalaiwe, The clinical pharmacokinetics impact of medical nanometals on drug delivery system, Nanomedicine 17 (2019) 47–61.
[2] J. Liu, J. Dong, T. Zhang, Q. Peng, Graphene-based nanomaterials and their potentials in advanced drug delivery and cancer therapy, J. Control. Release 286 (2018) 64–73.
[3] W. Liao, Y. Du, C. Zhang, F. Pan, Y. Yao, T. Zhang, Q. Peng, Exosomes: the next generation of endogenous nanomaterials for advanced drug delivery and therapy, Acta Biomater. 86 (2019) 1–14.
[4] M.J. Ernsting, M. Murakami, A. Roy, S.D. Li, Factors controlling the pharmacokinetics, biodistribution and intratumoral penetration of nanoparticles, J. Control. Release 172 (2013) 782–794.
[5] Y.N. Zhang, W. Poon, A.J. Tavares, I.D. McGilvray, W.C.W. Chan, Nanoparticle-liver interactions: cellular uptake and hepatobiliary elimination, J. Control. Release 240 (2016) 332–348.
[6] H. Wang, C.A. Thorling, X. Liang, K.R. Bridle, J.E. Grice, Y. Zhu, D.H.G. Crawford, Z.P. Xu, X. Liu, M.S. Roberts, Diagnostic imaging and therapeutic application of nanoparticles targeting the liver, J. Mater. Chem. B 3 (2015) 939–958.
[7] L.T. Hoekstra, W. de Graaf, G.A. Nibourg, M. Heger, R.J. Bennink, B. Stieger, T.M. van Gulik, Physiological and biochemical basis of clinical liver function tests: a review, Ann. Surg. 257 (2013) 27–36.
[8] M.K. Rasmussen, L. Bertholdt, A. Gudiksen, H. Pilegaard, J.G. Knudsen, Impact of fasting followed by short-term exposure to interleukin-6 on cytochrome P450 mRNA in mice, Toxicol. Lett. 282 (2018) 93–99.
[9] J.G. Lamb, L.B. Hathaway, M.A. Munger, J.L. Raucy, M.R. Franklin, Nanosilver particle effects on drug metabolism in vitro, Drug Metab. Dispos. 38 (2010) 2246–2251.
[10] Y. Zhang, Y. Wang, A. Liu, S.L. Xu, B. Zhao, Y. Zhang, H. Zou, W. Wang, H. Zhu, B. Yan, Modulation of carbon nanotubes' perturbation to the metabolic activity of CYP3A4 in the liver, Adv. Funct. Mater. 26 (2016) 841–850.
[11] L. Qiu, Q. Li, J. Huang, Q. Wu, K. Tu, Y. Wu, X. Zhang, J. Qian, R. Zhang, G. Li, M. Sun, L. Si, In vitro effect of mPEG2k-PCLx micelles on rat liver cytochrome P450 enzymes, Int. J. Pharm. 552 (2018) 99–110.
[12] X. Ke, V.W. Ng, R.J. Ono, J.M. Chan, S. Krishnamurthy, Y. Wang, J.L. Hedrick, Y.Y. Yang, Role of non-covalent and covalent interactions in cargo loading capacity and stability of polymeric micelles, J. Control. Release 193 (2014) 9–26.
[13] H. Cabral, K. Miyata, K. Osada, K. Kataoka, Block copolymer micelles in nanomedicine applications, Chem. Rev. 118 (2018) 6844–6892.
[14] A. Gothwal, I. Khan, U. Gupta, Polymeric micelles: recent advancements in the delivery of anticancer drugs, Pharm. Res. 33 (2016) 18–39.
[15] M. Ukawala, T. Rajyaguru, K. Chaudhari, A.S. Manjappa, S. Pimple, A.K. Babbar, R. Mathur, A.K. Mishra, R.S. Murthy, Investigation on design of stable etoposide-loaded PEG-PCL micelles: effect of molecular weight of PEG-PCL diblock copolymer on the in vitro and in vivo performance of micelles, Drug Deliv. 19 (2012) 155–167.
[16] J. Liu, F. Zeng, C. Allen, In vivo fate of unimers and micelles of a poly(ethylene glycol)-block-poly(caprolactone) copolymer in mice following intravenous administration, Eur. J. Pharm. Biopharm. 65 (2007) 309–319.
[17] S. Kim, Y. Shi, J.Y. Kim, K. Park, J.-X. Cheng, Overcoming the barriers in micellar drug delivery: loading efficiency, in vivo stability, and micelle–cell interaction, Expert Opin. Drug Discov. 7 (2010) 49–62.
[18] L. Qiu, L. Si, K. Tu, Q. Wu, G. Li, J. Huang, M. Sun, Effect of mPEG-PLGA polymer on the activity of rat CYP450 isozymes in vitro, Chin. Hosp. Pharm. J. 36 (2016) 1276–1282.
[19] N.-V. Cuong, M.-F. Hsieh, Y.-T. Chen, I. Liau, Synthesis and characterization of PEG-PCL-PEG triblock copolymers as carriers of doxorubicin for the treatment of breast cancer, J. Appl. Polym. Sci. 117 (2010) 3694–3703.
[20] X. Wang, Z. Wu, J. Li, G. Pan, D. Shi, J. Ren, Preparation, characterization, biotoxicity, and biodistribution of thermo-responsive magnetic complex micelles formed by Mn0.6Zn0.4Fe2O4 and a PCL/PEG analogue copolymer for controlled drug delivery, J. Mater. Chem. B 5 (2017) 296–306.
[21] K. Xiao, Y. Li, J. Luo, J.S. Lee, W. Xiao, A.M. Gonik, R.G. Agarwal, K.S. Lam, The effect of surface charge on in vivo biodistribution of PEG-oligocholic acid based micellar nanoparticles, Biomaterials 32 (2011) 3435–3446.
[22] P. Grossen, D. Witzigmann, S. Sieber, J. Huwyler, PEG-PCL-based nanomedicines: a biodegradable drug delivery system and its application, J. Control. Release 260 (2017) 46–60.
[23] P. Zhang, X. Yang, Y. He, Z. Chen, B. Liu, C.S. Emesto, G. Yang, W. Wang, J. Zhang, R. Lin, Preparation, characterization and toxicity evaluation of amphotericin B loaded MPEG-PCL micelles and its application for buccal tablets, Appl. Microbiol. Biotechnol. 101 (2017) 7357–7370.
[24] K.B. Knudsen, H. Northeved, P.E. Kumar, A. Permin, T. Gjetting, T.L. Andresen, S. Larsen, K.M. Wegener, J. Lykkesfeldt, K. Jantzen, S. Loft, P. Moller, M. Roursgaard, In vivo toxicity of cationic micelles and liposomes, Nanomedicine 11 (2015) 467–477.
[25] H.Q. Tang, M. Xu, Q. Rong, R.W. Jin, Q.J. Liu, Y.L. Li, The effect of ZnO nanoparticles on liver function in rats, Int. J. Nanomed. 11 (2016) 4275–4285.
[26] R. Ramakrishna, M. Bhateria, R. Singh, R.S. Bhatta, Evaluation of the impact of 16-dehydropregnenolone on the activity and expression of rat hepatic cytochrome P450 enzymes, J. Steroid Biochem. Mol. Biol. 163 (2016) 183–192.
[27] Z. Song, W. Zhu, J. Song, P. Wei, F. Yang, N. Liu, R. Feng, Linear-dendrimer type methoxy-poly (ethylene glycol)-b-poly (epsilon-caprolactone) copolymer micelles for the delivery of curcumin, Drug Deliv. 22 (2015) 58–68.
[28] M. Cagel, F.C. Tesan, E. Bernabeu, M.J. Salgueiro, M.B. Zubillaga, M.A. Moretton, D.A. Chiappetta, Polymeric mixed micelles as nanomedicines: achievements and perspectives, Eur. J. Pharm. Biopharm. 113 (2017) 211–228.
[29] H. Cabral, K. Kataoka, Progress of drug-loaded polymeric micelles into clinical studies, J. Control. Release 190 (2014) 465–476.
[30] C. Allen, D. Maysinger, A. Eisenberg, Nano-engineering block copolymer aggregates for drug delivery, Colloids Surf. B Biointerf. 16 (1999) 3–27.
[31] K. Letchford, R. Liggins, K.M. Wasan, H. Burt, In vitro human plasma distribution of nanoparticulate paclitaxel is dependent on the physicochemical properties of poly (ethylene glycol)-block-poly(caprolactone) nanoparticles, Eur. J. Pharm. Biopharm. 71 (2009) 196–206.
[32] X. Sun, G. Wang, H. Zhang, S. Hu, X. Liu, J. Tang, Y. Shen, The Blood clearance kinetics and pathway of polymeric micelles in cancer drug delivery, ACS Nano (2018).
[33] S. Stolnik, C.R. Heald, J. Neal, M.C. Garnett, S.S. Davis, L. Illum, S.C. Purkis, R.J. Barlow, P.R. Gellert, Polylactide-poly(ethylene glycol) micellar-like particles as potential drug carriers: production, colloidal properties and biological performance, J. Drug Target. 9 (2001) 361–378.
[34] V. Tzankova, C. Gorinova, M. Kondeva-Burdina, R. Simeonova, S. Philipov, S. Konstantinov, P. Petrov, D. Galabov, K. Yoncheva, In vitro and in vivo toxicity evaluation of cationic PDMAEMA-PCL-PDMAEMA micelles as a carrier of curcumin, Food Chem. Toxicol 97 (2016) 1–10.
[35] R. Jover, R. Bort, M.J. Gómez-Lechón, J.V. Castell, Down-regulation of human CYP3A4 by the inflammatory signal interleukin 6: molecular mechanism and transcription factors involved, FASEB J. 16 (2002) 1799–1801.
[36] A.E. Aitken, T.A. Richardson, E.T. Morgan, Regulation of drug-metabolizing enzymes and transporters in inflammation, Annu. Rev. Pharmacol. Toxicol. 46 (2006) 123–149.
[37] M.A.K. Abdelhalim, B.M. Jarrar, Histological alterations in the liver of rats induced by different gold nanoparticle sizes, doses and exposure duration, J. Nanobiotechnol. 10 (2012) 5.
[38] H. Zhang, L. Zhou, J. Yuen, N. Birkner, V. Leppert, P.A. O'Day, H.J. Forman, Delayed Nrf2-regulated antioxidant gene induction in response to silica nanoparticles, Free Radic. Biol. Med. 108 (2017) 311–319.
[39] R. Wu, Z. Xiao, X. Zhang, F. Liu, W. Zhou, Y. Zhang, The Cytochrome P450-mediated metabolism alternation of four effective lignans from schisandra chinensis in carbon tetrachloride-intoxicated rats and patients with advanced hepatocellular carcinoma, Front Pharmacol. 9 (2018) 229.
[40] J. Venhorst, A.M. ter Laak, J.N. Commandeur, Y. Funae, T. Hiroi, N.P. Vermeulen, Homology modeling of rat and human cytochrome P450 2D (CYP2D) isoforms and computational rationalization of experimental ligand-binding specificities, J. Med. Chem. 46 (2003) 74–86.
[41] S. Narimatsu, D. Kazamori, K. Masuda, T. Katsu, Y. Funae, S. Naito, H. Nakura, S. Yamano, N. Hanioka, The mechanism causing the difference in kinetic properties between rat CYP2D4 and human CYP2D6 in the oxidation of dextromethorphan and bufuralol, Biochem. Pharmacol. 77 (2009) 920–931.
[42] O. Videau, S. Pitarque, S. Troncale, P. Hery, E. Thevenot, M. Delaforge, H. Benech, Can a cocktail designed for phenotyping pharmacokinetics and metabolism enzymes in human be used efficiently in rat? Xenobiotica 42 (2012) 349–354.
[43] J.X. Zhang, M.J. Qi, M.Z. Shi, J.J. Chen, X.Q. Zhang, J. Yang, K.Z. Zhang, Y.L. Han, C. Guo, Effects of Danhong injection, a traditional Chinese medicine, on nine cytochrome P450 isoforms in vitro, Biomed. Chromatogr. 33 (2019) e4454.
[44] R. Zuber, E. Anzenbacherova, P. Anzenbacher, Cytochromes P450 and experimental models of drug metabolism, J. Cell Mol. Med. 6 (2002) 189–198.
[45] H. Komura, M. Iwaki, Species differences in in vitro and in vivo small intestinal metabolism of CYP3A substrates, J. Pharm. Sci. 97 (2008) 1775–1800.
[46] S. Roller, D. Cui, C. Laspina, C. Miller-Stein, J. Rowe, B. Wong, T. Prueksaritanont, Preclinical pharmacokinetics of MK-0974, an orally active calcitonin-gene related peptide (CGRP)-receptor antagonist, mechanism of dose dependency and species differences, Xenobiotica 39 (2009) 33–45.
[47] Q. Peng, H. Mu, The potential of protein-nanomaterial interaction for advanced drug delivery, J. Control. Release 225 (2016) 121–132.
[48] M. Ye, L. Tang, M. Luo, J. Zhou, B. Guo, Y. Liu, B. Chen, Size-and time-dependent alteration in metabolic activities of human hepatic cytochrome P450 isozymes by gold nanoparticles via microsomal coincubations, Nanoscale Res. Lett. 9 (2014) 642.
[49] A. Sereemaspun, P. Hongpiticharoen, R. Rojanathanes, P. Maneewattanapinyo, S. Ekgasit, W. Warisnoicharoen, Inhibition of human cytochrome P450 enzymes by metallic nanoparticles: a preliminary to nanogenomics, Int. J. Pharmacol. 4 (2008) 492–495.
[50] Y. Takakura, R.I. Mahato, M. Hashida, Extravasation of macromolecules, Adv. Drug Deliv. Rev. 34 (1998) 93–108.
[51] M. Gaumet, A. Vargas, R. Gurny, F. Delie, Nanoparticles for drug delivery: the need for precision in reporting particle size parameters, Eur. J. Pharm. Biopharm. 69 (2008) 1–9.

[52] H. Ruh, B. Kuhl, G. Brenner-Weiss, C. Hopf, S. Diabate, C. Weiss, Identification of serum proteins bound to industrial nanomaterials, Toxicol. Lett. 208 (2012) 41–50.
[53] S.R. Saptarshi, A. Duschl, A.L. Lopata, Interaction of nanoparticles with proteins: relation to bio-reactivity of the nanoparticle, J. Nanobiotechnol. 11 (2013) 26.
[54] M.A. Munger, G. Hadlock, G. Stoddard, M.H. Slawson, D.G. Wilkins, N. Cox, D. Rollins, Assessing orally bioavailable commercial silver nanoparticle product on human cytochrome P450 enzyme activity, Nanotoxicology 9 (2014) 474–481.
[55] J.K. Park, T. Utsumi, Y.E. Seo, Y. Deng, A. Satoh, W.M. Saltzman, Y. Iwakiri, Cellular distribution of injected PLGA-nanoparticles in the liver, Nanomedicine 12 (2016) 1365–1374.
[56] D. Spaggiari, L. Geiser, Y. Daali, S. Rudaz, A cocktail approach for assessing the in vitro activity of human cytochrome P450s: an overview of current methodologies, J. Pharm. Biomed. Anal. 101 (2014) 221–237.
[57] H. Tang, M. Xu, F. Shi, G. Ye, C. Lv, J. Luo, L. Zhao, Y. Li, Effects and mechanism of nano-copper exposure on hepatic cytochrome P450 enzymes in rats, Int. J. Mol. Sci. 19 (2018).
[58] M. Xu, H. Tang, X. Zhou, H. Chen, Q. Dong, Y. Zhang, G. Ye, F. Shi, C. Lv, B. Jing, C. He, L. Zhao, Y. Li, Effects and mechanisms of sub-chronic exposure to copper nanoparticles on renal cytochrome P450 enzymes in rats, Environ. Toxicol. Pharmacol. 63 (2018) 135–146.
[59] J.H. Lin, CYP induction-mediated drug interactions: in vitro assessment and clinical implications, Pharm. Res. 23 (2006) 1089–1116.
[60] L. Zhou, M. Cui, L. Zhao, D. Wang, T. Tang, W. Wang, S. Wang, H. Huang, X. Qiu, Potential metabolic drug-drug interaction of citrus aurantium L. (Rutaceae) evaluating by its effect on 3 CYP450, Front Pharmacol. 9 (2018) 895–905.
[61] V. Nedelcheva, I. Gut, P450 in the rat and man: methods of investigation, substrate specificities and relevance to cancer, Xenobiotica 24 (1994) 1151–1175.
[62] T. Liu, W. Zhang, Z. Zhang, M. Chen, J. Wang, X. Qian, W. Qin, Sensitive western-blot analysis of azide-tagged protein post translational modifications using thermoresponsive polymer self-assembly, Anal. Chem. 90 (2018) 2186–2192.